The Journal of Experimental Biology 202, 2239–2244 (1999)
Printed in Great Britain © The Company of Biologists Limited 1999
JEB2008

ULTRASTRUCTURAL OBSERVATIONS OF ADHERENT CELL PAIRS IN *HYDRA VULGARIS*

YASUHARU TAKAKU[1,*], TAKAHIKO HARIYAMA[1], MASASHI KURACHI[2] AND YASUO TSUKAHARA[1,2]

[1]*Graduate School of Information Sciences, Tohoku University, 2-1-1 Katahira, Aoba, Sendai 980-8577, Japan* and [2]*Photodynamics Research Center, The Institute of Physical and Chemical Research (RIKEN), 19-1399 Koeji, Nagamachi, Aoba, Sendai 982-0842, Japan*

*e-mail: takaku@biology.is.tohoku.ac.jp

Accepted 27 May; published on WWW 9 August 1999

Summary

Previous morphological studies of cell sorting in *Hydra vulgaris* have considered only clusters of cells. Here, we present ultrastructural observations on the adherent region of cell pairs brought into contact (following dissociation) using a three-dimensional laser manipulator. There was a much larger area of close membrane contact between endodermal cell pairs in comparison with ectodermal cell pairs. Separation distances between membranes were categorized into three classes: closest distance (<4 nm); medium distance (5–25 nm); and cleavage (>25 nm). The sum of distances in the closest and medium categories as a proportion of total contact length was significantly greater (P<0.01) for endodermal cells (49.0±6.5 %) than for ectodermal cells (26.7±4.4 %). In intact *Hydra*, this sum of distances was also significantly greater for endodermal cells, indicating that newly adherent cells, even after adhesion for only 10 min, display similar morphological characteristics to cells in intact *Hydra*. This suggests that close membrane contacts contribute to differential cell adhesion, which may form the basis of the cell sorting process.

Key words: cell sorting, cell junction, cell contact, adhesion, *Hydra vulgaris.*

Introduction

Hydra vulgaris has a simple body plan consisting of two layers of cells, ectodermal and endodermal layers (e.g. Campbell and Bode, 1983), and has a strong regenerative capacity. There are many reports concerning the regeneration of *Hydra* (for a review, see Bode and Bode, 1984), either from a small piece cut from the whole animal (Shimizu et al., 1993) or from a cell aggregate produced from dissociated single cells (Noda, 1971; Gierer et al., 1972).

In aggregates of *Hydra*, in which the original body plan has been destroyed, a process of cell sorting (for a review, see Armstrong, 1989) contributes to the formation of a new body pattern by separating the ectodermal from the endodermal cells (Gierer et al., 1972). The driving force for the sorting process in *Hydra* appears to be a differential adhesiveness (Technau and Holstein, 1992; originally proposed by Steinberg, 1970), which explains why cells can rearrange themselves into the most stable pattern from an initially random cell mass. Overton (1977), using aggregates derived from chick and mouse cells, suggested that differences in adhesive force between cells could control cell sorting and that this sorting was related to the density of cell junctions. When old cells, which form many junctions, are combined with young cells, which form few, cells with the highest capacity for junction formation are sorted into the interior of the aggregate.

The adhesive forces between dissociated *Hydra* epithelial cells have been measured (Sato-Maeda et al., 1994) using a three-dimensional laser manipulator for individual cells (Tashiro et al., 1993). The adhesive force is greater between endodermal epithelial cell pairs (>50 pN) than between ectodermal epithelial cell pairs (approximately 30 pN). Sato-Maeda et al. (1994) hypothesized that differences in adhesive forces among single, isolated cells could contribute to the initiation of cell sorting.

The results presented here demonstrate the ultrastructural characteristics of the adherent region of endodermal and ectodermal cell pairs, which had been dissociated from intact *Hydra* and allowed to re-adhere. The differences between the adherent regions of endodermal and ectodermal cell pairs are analyzed.

Materials and methods

Animals and cellular dissociation

Hydra vulgaris (cell line K9), provided by Professor Sugiyama (National Institute of Genetics, Japan), were used for all experiments. Stock cultures of animals were maintained in a *Hydra* culture medium, ‘M’ solution (Sugiyama and Fujisawa, 1977) at a constant temperature of 18 °C. Animals were fed on newly hatched brine shrimp nauplii six times per week. After the culture water had been renewed, experimental

animals were starved for 24 h prior to cellular dissociation to avoid the debris of brine shrimp nauplii.

Isolated cells were collected from 15 *Hydra* bodies, from which the mouth and foot regions had been surgically removed, and minced into small fragments. Cells were then dissociated mechanically by repeated pipetting in a hyperosmotic dissociation medium (DM; Flick and Bode, 1983). After filtration through mesh (45–53 μm pore size), cells were collected by low-speed centrifugation (80 ***g***), resuspended in 1 ml of fresh DM and filtered through mesh (37 μm pore size) to isolate single cells (Sato-Maeda et al., 1994).

Preparation for transmission electron microscopy

Dissociated cells in 1 ml of DM in a sample chamber, which was surface-coated with 0.35 % agar, were placed on the stage of a three-dimensional laser manipulator (Tashiro et al., 1993). An isolated single cell was lifted and transported by laser beam to a micropipette, where the cell was clamped by suction. Another isolated single cell was then transported by laser beam to a position above the first cell and pushed down to make good contact. After 30 s of forced contact, the laser beams were switched off and the cell pair was assessed to determine whether the cells remained adherent or separated (Sato-Maeda et al., 1994). Ten minutes after the forced contact, fixation of the cells for transmission electron microscopy was initiated using concentric double pipettes (Fig. 1A).

The fixation procedure is illustrated in Fig. 1B: transfer of cells to different solutions is performed while maintaining an aqueous environment, that is, avoiding exposure to air. Fixation was for 2 h in 2.5 % glutaraldehyde and 2 % paraformaldehyde in 0.1 mol l^{-1} phosphate buffer (pH 7.4), followed by three washes of 10 min each in 0.1 mol l^{-1} phosphate buffer (pH 7.4) containing 4 % sucrose. The cells were then postfixed for 30 min in ice-cold 2 % OsO_4 in the same buffer and washed three times for 10 min each in ice-cold distilled water. The cells were then dehydrated through a graded series of ethanol solutions. While cells were dehydrating in 100 % ethanol, they were mechanically removed from the head of the inner pipette under a dissection microscope, before final dehydration in propylene oxide and embedding in Epon Araldite mixture. Ultrathin (approximately 50 nm) sections were cut in the plane of attachment of the adhering cells and stained with 2 % uranyl acetate followed by 0.4 % lead citrate for 5 min each. Five serial sections of the widest adherent region were observed for each of five pairs of adherent cells (25 sections in total) using a transmission electron microscope (Hitachi H-300).

Results

Observations on the adherent region of cell pairs

One section of a pair of endodermal cells after for 10 min adhesion is shown in Fig. 2. The free membrane surface of adhering cell pairs showed irregularities in the electron microscopic observation. The adherent region was smooth and flat in comparison with the free cell surface.

Fig. 3 shows the adherent region of endodermal epithelial cells approximately 25 μm in diameter. The membrane contact is close and complex over a total contact length of approximately 3.2 μm. This contact length was observed to range from 2.7 μm to 9.2 μm (5.3±0.8 μm; mean ± S.E.M.). The membranes of adherent pairs of endodermal cells exhibited several separation distances. The closest separation distance between membranes was less than 4 nm (arrowheads). Arrows indicate medium separation distances (approximately 5–25 nm; 64.3 % of these distances were 15–20 nm). Cleavages much

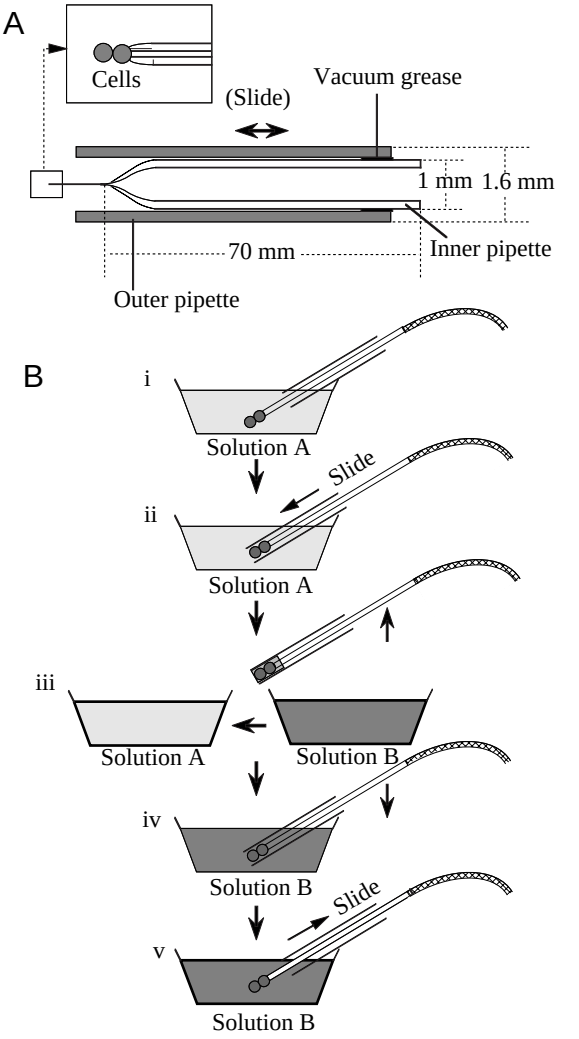

Fig. 1. (A) Schematic drawing of the concentric double pipettes designed to maintain an aqueous environment and to avoid surface tension damage to adherent cell pairs. The inner pipette holds a cell by suction and the outer pipette slides to cover the cell pair. (B) Fixation procedure for adherent cells held on the tip of the inner pipette in a sample chamber (i). (ii) The outer pipette is extended over the tip of the inner pipette to enclose the cells in solution (solution A). (iii) The double pipette is used to transfer the cells between fixative solutions (from solution A to solution B). (iv) The tip of a double pipette is immersed in the fixative solution (solution B). (v) Fixation of adhered cells begins when the outer pipette is slid back.

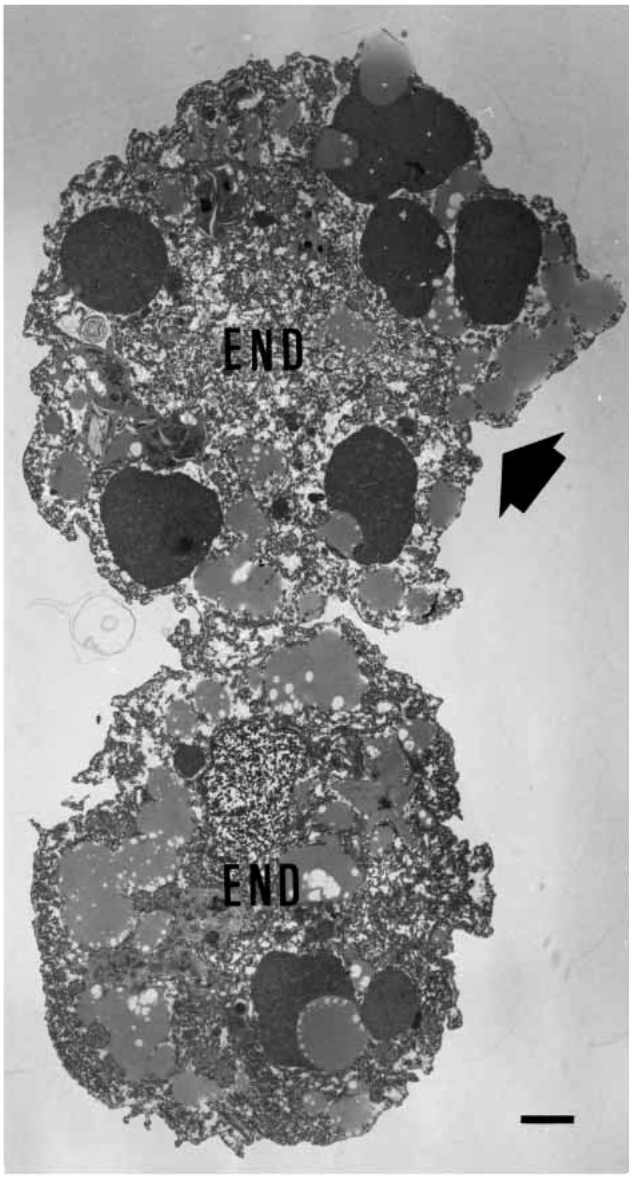

Fig. 2. Two single endodermal epithelial cells (END) of *Hydra* after adhesion for 10 min. The arrow indicates the region that was held by the inner pipette. Scale bar, 2 μm.

wider than 25 nm were also observed (asterisks) with low electron opacity.

The adherent region of ectodermal epithelial cells showed smooth and straight membrane contact. The cells were each approximately 10 μm in diameter, and the total contact length between cell pairs was approximately 1.6 μm (Fig. 4). Observed contact length ranged from 1.3 μm to 3.6 μm (1.8±0.9 μm; mean ± S.E.M.). In comparison with endodermal cell pairs, there were far fewer instances of the closest separation distance between membranes (Fig. 4, arrowheads). Many instances of medium separation distances of 5–25 nm (Fig. 4, arrows; 72 % of these distances were 15–20 nm) were also observed in the adherent regions. There was no filament-like structure in the intracellular space between either

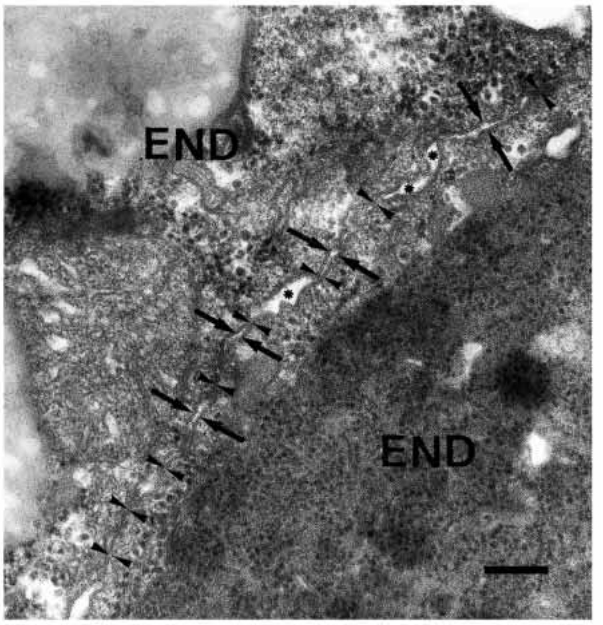

Fig. 3. High-resolution micrograph of the adherent region between a pair of endodermal cells (END) showing several classes of separation distance between adjacent cell membranes. Arrowheads indicate the closest separation distance, less than 4 nm. Arrows indicate the medium separation distance of 5–25 nm. Separation distances much greater than 25 nm are also observed (asterisks), and are associated with the low electron opacity. Scale bar, 200 nm.

ectodermal or endodermal cell pairs. The adhesion of endodermal and ectodermal cell pairs was not observed within 30 s of forced contact in this study.

Quantitative analysis of the separation distance for adhering cell pairs and for intact Hydra

Separation distances were compared for endodermal and ectodermal adherent cell pairs (Fig. 5A). The proportions of different separation distances for cell pairs are shown in Fig. 5B. The percentage of closest separation distances between endodermal cells (22.8±3.8 %; mean ± S.E.M., N=25) was significantly greater (Student's t-test; P<0.01) than that for ectodermal cells (10.3±2.3 %) (Fig. 5B). The sum of distances in the closest and medium categories as a proportion of total contact length was significantly greater (P<0.01) in endodermal cells (49.0±6.5 %) than in ectodermal cells (26.7±4.4 %).

We also analyzed the separation distances between membranes in the middle of the body of intact *Hydra* in the same manner as for adherent cells (three serial sections, selected at random from the body length from five independent animals; 15 sections in total). Membrane contact between endodermal cells was close and complex, with a total contact length of 67.7±6.3 μm, whereas for ectodermal cells it was smooth and straight, with a total contact length of 29.4±7.2 μm (Fig. 6A). There was a greater difference in the separation distance proportions between endodermal and ectodermal cells in intact *Hydra* (Fig. 6B) than in dissociated *Hydra*. In intact

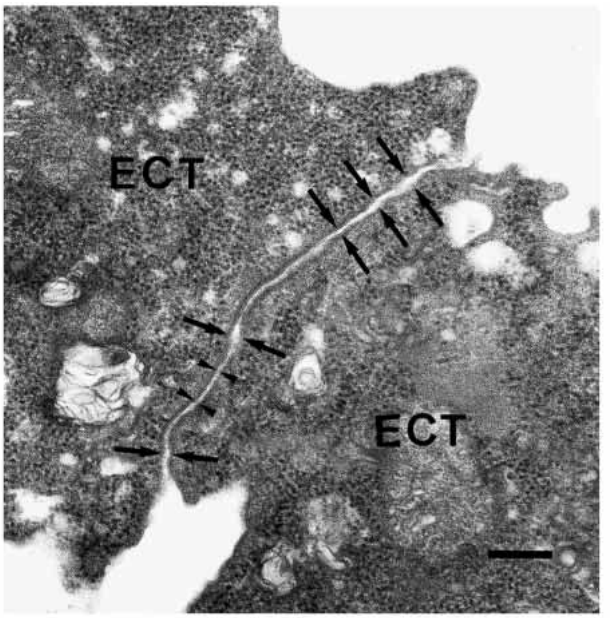

Fig. 4. One section of the area of closest membrane contact in the adherent region between ectodermal epithelial cells (ECT), showing the closest separation distance between membranes (arrowheads) and the medium separation distance (arrows). Scale bar, 200 nm.

Hydra, the percentage of closest separation distances was significantly greater (P<0.01) in endodermal cells (26.6±2.1 %) than in ectodermal (10.8±2.2 %) cells. The sum of the distances in the closest and medium categories as a proportion of total contact length for intact *Hydra* was significantly greater (P<0.01) in endodermal cells (84.4±3.1 %) than in ectodermal (61.4±7.8 %) cells.

Discussion

The freshwater polyp *Hydra vulgaris* has been used extensively in regeneration experiments (for a review, see Berking, 1997). Even aggregates of single cells can transform into normal-shaped animals (Noda, 1971; Gierer et al., 1972). The regeneration process from aggregates has been examined at several stages; cell-to-cell interaction (Sato-Maeda et al., 1994), cell rearrangement (Technau and Holstein, 1992), cell-to-extracellular matrix interaction (Sarras et al., 1994) and morphogenesis (Sarras et al., 1992). Kishimoto et al. (1996) suggested that radial cell interactions at the contact surface play a crucial role in producing ectodermal spreading and epithelial sheet organization in the recombined aggregates.

The active process of cell sorting is the initial process of cell rearrangement. In several species, transformation of an initially disordered array of cohering cells into one in which the cells are organized into homogeneous tissue domains is a crucial early process (for a review, see Armstrong, 1989). One of the widely accepted properties of the sorting process is the characteristic adhesive strength, which depends on tissue specificity (the differential adhesion hypothesis, originally proposed by Steinberg, 1970). Wood and Kuda (1980) found that septate junctions, which are a candidate for estimation of adhesive force, are reorganized by 4 h after reaggregation. We focused here on the origin of adhesive force in the early regeneration process using morphological observation of single dissociated cell pairs.

Although single cells have previously been manoeuvred using a three-dimensional laser manipulator (Tashiro et al., 1993), and the adhesive forces determined between newly adhered dissociated *Hydra* epithelial cells (Sato-Maeda et al., 1994), the adherent cells were too small to handle under on ordinary electron microscopy using routine methods. It was therefore necessary to establish a new technique to control and fix cell pairs over a closely controlled adhesion time. The double-pipette method solved the problems of handling such small cells for electron microscopy.

In intact *Hydra*, the following separation distances were distinguished: (1) less than 4 nm, which includes gap junctions (Wood, 1977); (2) approximately 15–25 nm, which includes septate junctions (Wood, 1959), fascial intermediate junctions (Wood, 1977) and interdigitations (West, 1978); and (3) distances much greater than 25 nm, which are considered not

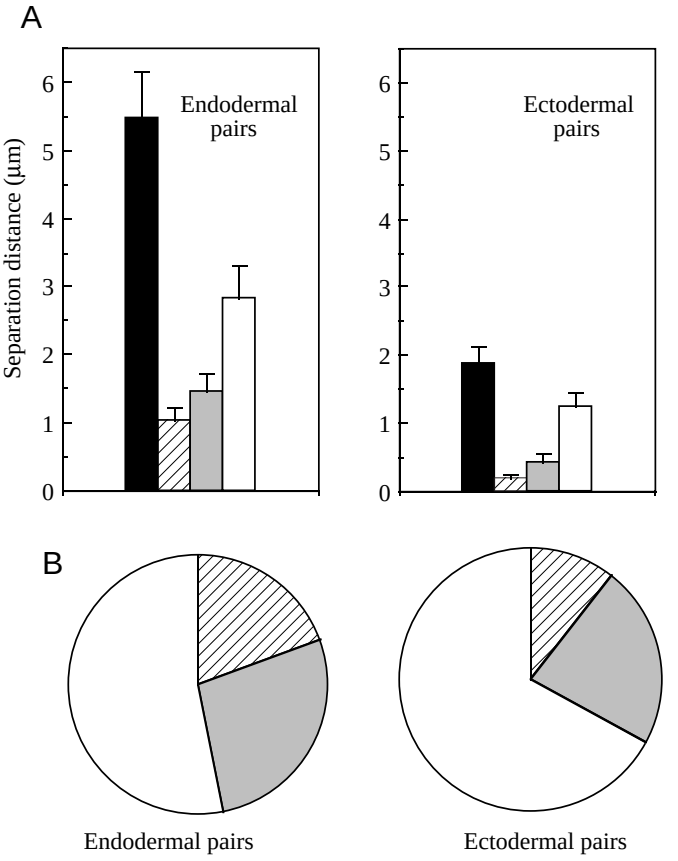

Fig. 5. Analysis of separation distances of adherent regions of endodermal and ectodermal cells. (A) Histogram of mean values + S.E.M. (N=25). Hatched columns, <4 nm; grey columns, 5–25 nm; open columns, >25 nm; filled black columns, total contact length. (B) Separation distances expressed as a proportion of total contact length (shading as in A).

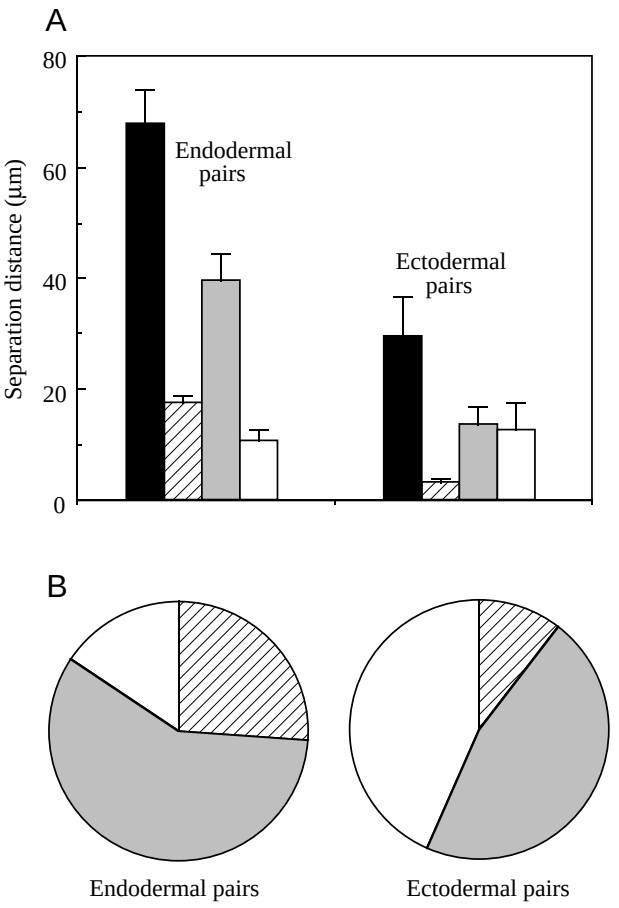

Fig. 6. (A) Analysis of separation distances between adherent membranes of intact *Hydra*. Hatched columns, <4 nm; grey columns, 5–25 nm; open columns, >25 nm; filled black columns, total contact length. Values are means + S.E.M., *N*=15. (B) Separation distances expressed as a proportion of total contact length (shading as in A).

to constitute cell junctions. The correspondence of the categorization into three classes of separation distance between intact *Hydra* and adherent cell pairs indicates that cell pairs, after only 10 min of adhesion, may already have adhesion properties similar to those in intact *Hydra*.

The proportion of closest distances (<4 nm) was significantly greater in endodermal cell pairs than in ectodermal cell pairs (Fig. 5B). In intact *Hydra*, gap junctions do not fracture in a conventional manner (Wood, 1977), implying that gap junctions in intact *Hydra* are held together by strong adhesive forces. Therefore, a large proportion of closest distances in adherent endodermal cells may increase considerably the strength of cell-to-cell adhesion. The sum of distances in the closest and medium categories as a proportion of total contact length in adherent cell pairs is considered to contribute to total cell adhesion, since both categories are also observed in intact *Hydra* (Wood, 1959, 1977; West, 1978). This sum was also significantly greater in endodermal than in ectodermal cell pairs (Fig. 5B).

We also calculated the separation distances in intact *Hydra* using the classification described above (Fig. 6A). The proportion of the closest distance (<4 nm) for endodermal cells was greater than that for ectodermal cells, and the sum of the distances in the closest and medium categories was also significantly greater than that for ectodermal cells (Fig. 6B). These results were similar to those obtained in adherent isolated cells (Fig. 5), suggesting that adherent cells have similar morphological characteristics to those of intact *Hydra*.

In intact *Hydra*, myofilaments are aggregated into bundles forming myonemes within the basal cytoplasm of the cell body in contact with the mesogloea (West, 1978). Dissociated single cells, except for nematoblasts, are spherical, as opposed to the normal elongated appearance of cells from intact animals in the light microscope (Noda, 1971). Adherent cell pairs also retain the smooth spherical shape observed in the light microscope in our study (data not shown). The surface of paired cells, however, appeared irregular using transmission electron microscopy (Fig. 2). High osmotic pressure is necessary to dissociate and maintain viable cells (Flick and Bode, 1983), and there is a possibility that these cell-surface irregularities were caused by high osmotic pressure. However, the cells in contact showed clear adhesiveness. No filament-like structures were observed gathering between either ectodermal or endodermal adherent cell pairs (Figs 3, 4), probably because of the loss of cell polarity after dissociation.

All adherent cell pairs observed in the electron microscope showed an irregular surface; however, the adherent region was smooth and flat (Fig. 2). Although the membranes of adherent cell pairs exhibited a range of separation distances (Figs 3, 4), the proportion of separation distances was different for endodermal and ectodermal cell pairs (Fig. 5B). The adhesion process of endodermal cell pairs was observed after 10, 20 and 60 min of adhesion. The proportion of close separation distances to total contact length showed a tendency to approach that of intact *Hydra* (Y. Takaku, in preparation). These results strongly suggest that, after only 10 min of adhesion, cell pairs have already started to acquire the same adhesive properties as those in intact *Hydra* and that adherent cell pairs are not merely touching but are adhering through specialized cell junctions.

Overton (1977) reported that the pattern of cell sorting is consistent with the pattern of junction formation: cells that form many junctions sort to the inner regions of the aggregate. He also pointed out that differences in adhesive force could control cell sorting, depending on the density of cell junctions. Adhesive force is greater between endodermal cell pairs (>50 pN; Sato-Maeda et al., 1994) than between ectodermal cell pairs (30 pN). We observed a greater proportion close membrane contacts between endodermal cells than between ectodermal cells, corroborating Overton's (1977) observations and suggesting that close membrane contacts may play a role in the cell sorting process at a very early stage.

We combined the use of double pipettes with a three-dimensional laser manipulator to control single cells for morphological observation and to investigate cell-to-cell surface interactions. Our data indicate that single cells of

different tissue origins show morphological differences in cell contact in the early regeneration process.

We wish to express our thanks to our colleague in the Photodynamics Research Center (RIKEN) and to Dr Ian Gleadall for helpful suggestions and comments on the manuscript.

References

Armstrong, P. B. (1989). Cell sorting out: The self-assembly of tissues *in vitro*. *CRC Crit. Rev. Biochem. Mol. Biol.* **24**, 119–149.

Berking, S. (1997). Pattern formation in Hydrozoa. *Naturwissenschaften* **84**, 381–388.

Bode, P. M. and Bode, H. R. (1984). Patterning in hydra. In *Pattern Formation* (ed. G. M. Malacinski and S. V. Baryant), pp. 213–241. New York: Macmillan.

Campbell, R. D. and Bode, H. R. (1983). Terminology for morphology and cell types. In Hydra*: Research Methods* (ed. H. M. Lenhoff), pp. 5–14. New York, London: Plenum Press.

Flick, K. M. and Bode, H. R. (1983). Dissociated tissues into cells and development of *Hydra* from aggregated cells. In Hydra*: Research Methods* (ed. H. M. Lenhoff), pp. 251–260. New York, London: Plenum Press.

Gierer, A., Berking, S., Bode, H., David, C. N., Flick, K. M., Hansmann, G., Schalle, H. and Trenkner, E. (1972). Regeneration of *Hydra* from reaggregated cells. *Nature New Biol.* **239**, 98–101.

Kishimoto, Y., Murate, M. and Sugiyama, T. (1996). *Hydra* regeneration from recombined ectodermal and endodermal tissue. I. Epibolic ectodermal spreading is driven by cell intercalation. *J. Cell Sci.* **109**, 763–772.

Noda, K. (1971). Reconstitution of dissociated cells of hydra. *Zool. Mag.* **80**, 99–101.

Overton, J. (1977). Formation of junctions and cell sorting in aggregates of chick and mouse cells. *Dev. Biol.* **55**, 103–116.

Sarras, M. P., Jr, Huff, J. K. and Palmiter-Thomas, P. (1992). High molecular weight secretory products of the human pancreatic ductal epithelium and the effect of secretin on their discharge. *Pancreas* **2**, 132–143.

Sarras, M. P., Jr, Yan, L., Grens, A., Zhang, X., Agbas, A., Huff, J., St John, P. L. and Abrahamson, D. R. (1994). Cloning and biological function of laminin in *Hydra vulgaris*. *Dev. Biol.* **164**, 312–324.

Sato-Maeda, M., Uchida, M., Graner, F. and Tashiro, H. (1994). Quantitative evaluation of tissue-specific cell adhesion at the level of a single cell pair. *Dev. Biol.* **162**, 77–84.

Shimizu, H., Sawada, Y. and Sugiyama, T. (1993). Minimum tissue size required for hydra regeneration. *Dev. Biol.* **155**, 287–296.

Steinberg, M. S. (1970). Does differential adhesion govern self-assembly processes in histogenesis? Equilibrium configurations and the emergence of a hierarchy among populations of embryonic cells. *J. Exp. Zool.* **173**, 395–434.

Sugiyama, T. and Fujisawa, T. (1977). Genetic analysis of developmental mechanisms in hydra. I. Sexual reproduction of *Hydra magnipapillata* and isolation of mutants. *Dev. Growth Differ.* **19**, 187–200.

Tashiro, H., Uchida, M. and Sato-Maeda, M. (1993). Three-dimensional cell manipulator by means of optical trapping for the specification of cell-to-cell adhesion. *Optical Eng.* **32**, 2812–2817.

Technau, U. and Holstein, T. W. (1992). Cell sorting during the regeneration of *Hydra* from reaggregated cells. *Dev. Biol.* **151**, 117–127.

West, D. L. (1978). The epitheliomuscular cell of *Hydra*: its fine structure, three-dimensional architecture and relation to morphogenesis. *Tissue & Cell* **10**, 629–646.

Wood, R. (1959). Intercellular attachment in the epithelium of *Hydra* as revealed by electron microscopy. *J. Biophys. Biochem. Cytol.* **6**, 343–352.

Wood, R. L. (1977). The cell junctions of *Hydra* as viewed by freeze-fracture replication. *J. Ultrastruct. Res.* **58**, 299–315.

Wood, R. L. and Kuda, A. M. (1980). Formation of junctions in regenerating *Hydra*: septate junctions. *J. Ultrastruct. Res.* **70**, 104–117.